Sigurdsson, H., Leckie, R.M., Acton, G.D., et al., 1997
Proceedings of the Ocean Drilling Program, Initial Reports, Vol. 165

7. SITE 1002[1]

Shipboard Scientific Party[2]

HOLE 1002A

Position: 10°42.366′N, 65°10.179′W (Cariaco Basin)

Date occupied: 1645 hr, 13 February 1996

Date departed: 2100 hr, 13 February 1996

Time on hole: 4.25 hr (0.18 days)

Seafloor depth (drill-pipe measurement from rig floor, mbrf): 904.3

Total depth (drill-pipe measurement from rig floor, mbrf): 914.5

Distance between rig floor and sea level (m): 11.6

Water depth (drill-pipe measurement from sea level, m): 892.7

Penetration (mbsf): 10.2

Coring totals:
Type: APC; No: 1; Cored: 9.50 m; Recovered: 9.77 m (102.8%)

Formation:
Silty clay with nannofossils and foraminifers, diatom nannofossil mixed sediment, and nannofossil silty clay

Oldest sediment cored:
Depth (mbsf): 10.20
Nature: Nannofossil silty clay
Age: Pleistocene

HOLE 1002B

Position: 10°42.366′N, 65°10.179′W (Cariaco Basin)

Date occupied: 2100 hr, 13 February 1996

Date departed: 2130 hr, 13 February 1996

Time on hole: 0.5 hr (0.02 days)

Seafloor depth (drill-pipe measurement from rig floor, mbrf): 904.3

Total depth (drill-pipe measurement from rig floor, mbrf): 910.5

Distance between rig floor and sea level (m): 11.6

Water depth (drill-pipe measurement from sea level, m): 892.7

Penetration (mbsf): 6.2

Coring totals:
Type: APC; No: 1; Cored: 6.20 m; Recovered: 6.24 m (100.6%)

Formation:
Silty clay with nannofossils and foraminifers, diatom nannofossil mixed sediment, and nannofossil silty clay

Oldest sediment cored:
Depth (mbsf): 6.20
Nature: Nannofossil silty clay
Age: Pleistocene

HOLE 1002C

Position: 10°42.366′N, 65°10.166′W (Cariaco Basin)

Date occupied: 2130 hr, 13 February 1996

Date departed: 0930 hr, 14 February 1996

Time on hole: 12 hr (0.5 days)

Seafloor depth (drill-pipe measurement from rig floor, mbrf): 904.1

Total depth (drill-pipe measurement from rig floor, mbrf): 1074.2

Distance between rig floor and sea level (m): 11.5

Water depth (drill-pipe measurement from sea level, m): 892.6

Penetration (mbsf): 170.1

Coring totals:
Type: APC; No: 18; Cored: 170.10 m; Recovered: 185.50 m (109.1%)

Formation:
Silty clay with nannofossils and foraminifers, diatom nannofossil clayey mixed sediment, clay, and nannofossil silty clay

Oldest sediment cored:
Depth (mbsf): 170.10
Nature: Nannofossil silty clay
Age: Pleistocene

HOLE 1002D

Position: 10°42.368′N, 65°10.161′W (Cariaco Basin)

Date occupied: 0930 hr, 14 February 1996

Date departed: 2215 hr, 14 February 1996

Time on hole: 12.75 hr (0.53 days)

Seafloor depth (drill-pipe measurement from rig floor, mbrf): 904.8

Total depth (drill-pipe measurement from rig floor, mbrf): 1071.6

Distance between rig floor and sea level (m): 11.5

Water depth (drill-pipe measurement from sea level, m): 893.6

Penetration (mbsf): 166.8

Coring totals:
Type: APC; No: 12; Cored: 109.20 m; Recovered: 120.37 m (110.2%)
Type: XCB; No: 6; Cored: 57.60 m; Recovered: 41.82 m (73.1%)

Formation:
Silty clay with nannofossils and foraminifers, diatom nannofossil mixed sediment, clay, and nannofossil silty clay

Oldest sediment cored:
Depth (mbsf): 166.80

[1]Sigurdsson, H., Leckie, R.M., Acton, G.D., et al., 1997. *Proc. ODP, Init. Repts.,* 165: College Station, TX (Ocean Drilling Program).
[2]Shipboard Scientific Party is given in the list preceding the Table of Contents.

Nature: Nannofossil silty clay
Age: Pleistocene

HOLE 1002E

Position: 10°42.364′N, 65°10.155′W (Cariaco Basin)

Date occupied: 2215 hr, 14 February 1996

Date departed: 1230 hr, 15 February 1996

Time on hole: 14.25 hr (0.59 days)

Seafloor depth (drill-pipe measurement from rig floor, mbrf): 904.7

Total depth (drill-pipe measurement from rig floor, mbrf): 1068.7

Distance between rig floor and sea level (m): 11.6

Water depth (drill-pipe measurement from sea level, m): 893.1

Penetration (mbsf): 164.0

Coring totals:
Type: APC; No: 13; Cored: 115.80 m; Recovered: 122.37 m (105.8%)
Type: XCB; No: 5; Cored: 48.20 m; Recovered: 42.51 m (88.2%)

Formation:
Silty clay with nannofossils and foraminifers, diatom nannofossil clayey mixed sediment, clay, and nannofossil silty clay

Oldest sediment cored:
Depth (mbsf): 164.0
Nature: Nannofossil silty clay
Age: Pleistocene

Principal results: Site 1002 is located adjacent to DSDP Site 147 in the Cariaco Basin, a structural depression on the northern continental shelf of Venezuela, which has the distinction of being the second largest anoxic marine body in the world after the Black Sea. The presence of laminated, high-deposition rate (300 to >1000 m/m.y.) sediments and location in a climatically sensitive region of the tropical ocean made Cariaco Basin a prime drilling target during Leg 165 for high-resolution studies of geologically recent climate change.

A total of five holes were drilled at Site 1002, two of which were dedicated mudline cores taken for geochemical studies, and three more taken for high-resolution paleoclimatic reconstructions. Only the cores from Hole 1002C were split open onboard ship for preliminary descriptions and sampling. Following the cruise, all cores from Site 1002 were shipped to the Gulf Coast Repository in College Station, TX, where a special post-cruise sampling party later met from May 28 to June 2, 1996, to open and describe cores from the remaining two holes. Though barrel sheets for cores from Holes 1002D and 1002E are included in this site chapter, the bulk of the data and the discussion are based on shipboard observations of Hole 1002C and only the most preliminary conclusions can be drawn at this time.

Hole 1002C recovered a total of 170.1 m of mostly mixed, or hemipelagic sediments. The presence of *Emiliania huxleyi* at the base of the sequence suggests that all of the sediments fall within Zone CN15, or were deposited in the past 248,000 yr. This single biostratigraphic estimate is consistent with estimates based on extrapolating known sedimentation rates for the Holocene and last glacial back the length of the drilled sequence.

Sediments in Hole 1002C are generally dominated by terrigenous components with variable biogenic contributions of nannofossils, diatoms, and foraminifers. Much of the sediment is laminated, indicating deposition under largely anoxic, bioturbation-free conditions. Microbial methane is common in the sediment, resulting in expanded sections and development of gas voids in many of the cores upon retrieval. However, the quality and continuity of the cores appears to be very good to excellent as voids largely developed along bedding surfaces.

The sedimentary sequence at Site 1002 was assigned to one formal lithologic unit and eight subunits. Despite this degree of subdivision, there appear to be only about three major lithologies, which alternate in a semi-predictable fashion. The bulk of the sequence consists of nannofossil silty clay, olive gray to greenish gray in color, which appears to have been deposited under both anoxic (laminated) and oxic (massive) conditions. These sediments are punctuated periodically by episodes of bluish gray and yellowish brown clay deposition, laid down under clearly oxic conditions. Generally following this, deposition of diatom-rich, distinctly laminated sediment indicates strong upwelling, such as was experienced during the early Holocene in Subunit IB. Earlier periods of clay deposition, followed by accumulation of diatom-rich sediments, may similarly signal earlier periods of sea level rise with deglaciation. Shore-based efforts to develop a stratigraphy for this site will allow testing of this hypothesis and will provide the basis for high- to ultra-high-resolution investigations of late Quaternary tropical paleoenvironments in the months and years ahead.

BACKGROUND AND OBJECTIVES

Site 1002 is located adjacent to DSDP Site 147 in the Cariaco Basin (Fig. 1), a structural depression on the northern continental shelf of Venezuela, which is the second largest anoxic marine body in the world (after the Black Sea). Since the first coring attempts in the late 1950s, it has been known that the laminated sediments that accumulate in the Cariaco Basin are nearly undisturbed by bioturbation and contain well-preserved assemblages of both calcareous and siliceous microfossils. High sedimentation rates (300 to >1000 m/m.y.) and its

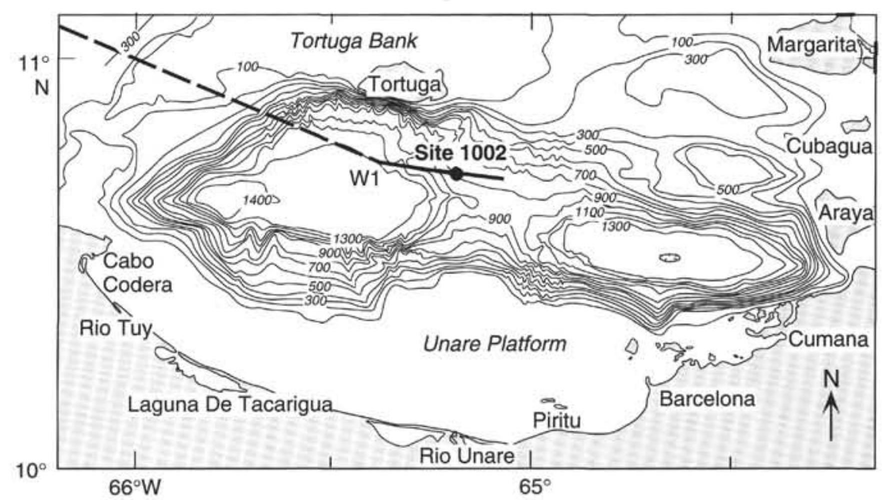

Figure 1. Bathymetry of Cariaco Basin showing location of Site 1002 on the central saddle that bisects the basin. Site 1002 is located at the approximate position of DSDP Site 147. The solid portion of the trackline, beginning at waypoint W-1, shows the approach of *JOIDES Resolution* from the west along an existing survey line from the PLUME-7 survey cruise (see "Seismic Stratigraphy" section, this chapter).

location in a climatically sensitive region of the tropical ocean made the Cariaco Basin a prime drilling target during Leg 165 for high-resolution studies of geologically recent climate change.

Today, upwelling of cold, nutrient-rich waters occurs along the northern Venezuelan coast in response to seasonal changes in the prevailing trade wind field, and varies in frequency and intensity in response to movement of the Intertropical Convergence Zone (ITCZ). The seasonal march of the ITCZ also causes variations in precipitation in northern South America that have a strong influence on the discharge of rivers that affect the western North Atlantic and southern Caribbean. Thus, sediments of the Cariaco Basin have the potential to reveal information about past changes in the circulation of the tropical atmosphere and ocean, and for the study of changes in the regional hydrologic balance over northern South America.

The major objectives at Site 1002 were to recover a continuous and undisturbed upper Quaternary stratigraphic section that will be used (1) to document how climate change in the southern Caribbean and northern South America relates to climatic-forcing mechanisms and to global-scale change, especially to high-latitude changes recorded in ice cores and high-deposition rate marine sediment sequences; (2) to study the rates and magnitudes of tropical climate change at interannual to millennial time scales over the last several glacial-interglacial cycles; (3) to examine the stability of tropical climate in response to past changes in large-scale global boundary conditions; and (4) to study the relationships between climate variability and processes that influence the burial of organic carbon in anoxic settings. Cariaco Basin sediments contain a rich array of proxy data sources that include calcareous and siliceous microfossil populations, pollen, organic carbon, terrigenous clays, and trace metals potentially used as geochemical proxies of export production and depositional redox. Analyzed together, they will offer the opportunity to reconstruct an exceptionally complete and highly resolved record of past changes in tropical climate and oceanic conditions.

A number of small basins occur in the boundary zone between the Caribbean Plate and the South American Plate. The Cariaco Basin, an area of largely fault-controlled recent sedimentation, is a pull-apart basin (Schubert, 1982) defined by the right-lateral strike-slip between the two plates along the Moron–Sebastian–El Pilar fault system. Rates of slip along these faults are on the order of 12–50 mm/yr, leading to a 25- to 100-km total offset in the Cariaco Basin since its formation about 2 m.y. ago (Mann et al., 1990; Ladd et al., 1990). The underlying basement is a complex mixture of metamorphosed slices or nappes of both plates, including ophiolites and metamorphic rocks of sedimentary and volcanic origin. The sediment thickness exceeds 1 km over much of the basin.

The Cariaco Basin is presently anoxic below about 300 m, a condition attributed to limited exchange of waters with the Caribbean across shallow inlet sills (~150 m) to the north and west through the Tortuga Bank, and excessive oxygen demand created by degradation of the high flux of organic detritus settling through the water column (see Richards [1975] and Peterson et al. [1991] for detailed discussions of the hydrography). The almost complete lack of bioturbation on the basin floor leads to preservation of a nearly undisturbed recent sediment record.

Heezen et al. (1958, 1959) were the first to report the characteristics of Cariaco Basin sediments based on 12 piston cores collected during a *Vema* cruise in 1957. Athearn (1965) later described a suite of more than 20 cores collected by the Woods Hole Oceanographic Institution in the early 1960s, whereas Lidz et al. (1969) contributed additional descriptions based on cores collected by the University of Miami in 1966. In 1970 on Deep Sea Drilling Project (DSDP) Leg 15, Site 147 was drilled by the *Glomar Challenger* on the western edge of the central saddle. The site survey for the present drilling effort was conducted in 1990 on Leg 7 of the PLUME Expedition (*Thomas Washington*), which also recovered a suite of 104 box, gravity, and piston cores from all parts and depths of the basin.

In the near-surface sediment column accessible by conventional piston coring, two major sediment units are typically found (Fig. 2). The upper anoxic unit consists of dark grayish green silty clays that are usually laminated, whereas the lower unit is composed of yellowish brown silty clays that are bioturbated and were clearly deposited under oxic bottom conditions. The transition between these two units has been radiocarbon dated at ~12.6 ka (Peterson et al., 1991). Below the oxic/anoxic transition, a distinctive, fine-grained gray clay layer is a pervasive feature in cores across the basin. In cores that are long enough, laminae reappear at the base suggesting an earlier phase of anoxic deposition.

Sediment laminae, where best developed in the upper anoxic unit, are millimeter to submillimeter scale in thickness and consist of light-dark sediment couplets. These couplets have been shown to reflect the seasonal cycle in surface hydrography, with diatom- and nannofossil-bearing sediment accumulation in the dry, upwelling season (winter–spring) and clay-rich accumulation in the wet, nonupwelling season (summer–fall). Their interpretation as annual varves, at least in the Holocene, is supported by ^{210}Pb analyses and Accelerator Mass Spectrometry ^{14}C dating (Hughen et al., 1996).

During DSDP Leg 15, a total of four holes were rotary drilled at Site 147, with the deepest penetration to 189 mbsf (Edgar, Saunders, et al., 1973). Hole 147 was devoted to sedimentologic and biostratigraphic studies and terminated at 162 mbsf. Holes 147A, 147B, and 147C were largely drilled for geochemical studies. The majority of cores from these holes were frozen, however, and never adequately described. Rotary coring, incomplete recovery, and the effects of gas (methane) expansion combined to produce a record too highly disturbed for high-resolution paleoceanographic studies. Overall, the sedimentary section at Site 147 was found to consist of a grayish olive calcareous clay similar in character to that described in piston cores and primarily deposited under anoxic conditions. Sediment laminations were reported to be visible at various depth levels in the section, although the disruptive nature of the rotary coring and the gassy nature of the sediments most likely prevented their preservation. Thin layers of brown and gray clay, thought by Leg 15 scientists to be comparable to oxic sediments deposited during the last glacial maximum, were observed at several deeper levels in the section, but

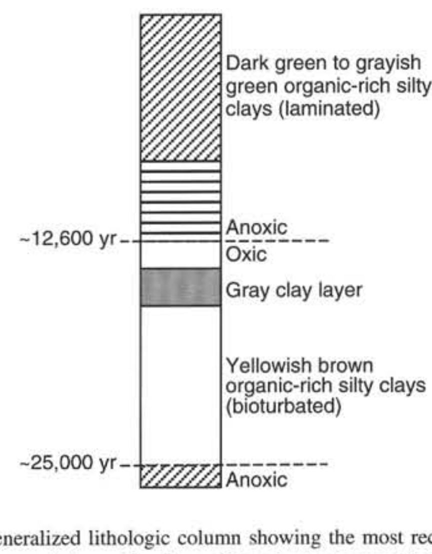

Figure 2. Generalized lithologic column showing the most recent transition from oxic to anoxic depositional conditions in the Cariaco Basin at ~12,600 ^{14}C yr ago (Peterson et al., 1991). The thickness of this upper anoxic unit generally ranges between 4 and 10 m across the basin. A return to laminated, anoxic sedimentation at the base of previously collected long piston cores, and observations from the badly disturbed DSDP Site 147, led to expectations before drilling that Site 1002 would recover similar laminated sequences over much of its length.

they could not be related to specific climatic events with the existing biostratigraphy.

Rögl and Bolli (1973) and Hay and Beaudry (1973) summarized the foraminiferal and calcareous nannofossil zonations of Site 147, respectively. By current standards, the age models for this site were very poor. Rögl and Bolli (1973) attempted to apply the *G. menardii* zonation scheme of Ericson and Wollin (1968) and concluded that sediments at the base of Hole 147 (162 mbsf) lie within the lower V zone of these authors. Extrapolation of sedimentation rates derived from the upper part of the section led them to assign an age of about 320 ka to the base of this hole.

Site 1002 is located at 10°42.37′N, 65°10.18′W on the western edge of the central saddle that bisects the Cariaco Basin into two smaller sub-basins (Fig. 1). The site was positioned on a flat, well-stratified sediment package just to the east of DSDP Site 147 at a water depth of 893 m. The operational plan at Site 1002 was to triple APC core the sediment section to a maximum depth of 180 mbsf. The presence of dolomite crusts at various sub-bottom levels and unusually firm sediments in Hole 1002C at depths below about 120 mbsf caused the APC to fail to achieve full-stroke, and necessitated a switch to XCB coring in Holes 1002D and 1002E to improve recovery and meet the site objectives. Holes 1002A and 1002B were mudline cores added to the drilling program to satisfy the objectives of the shipboard geochemists.

Site 1002 came at the very end of Leg 165, with approximately 2 days allocated to coring, followed by a short transit (~1.5 days) to the final port of San Juan, Puerto Rico. Because of the advance realization that normal processing of Site 1002 cores would not be possible in the available time, special provisions were made whereby only cores from the first of the long holes (1002C) would be opened on board for initial description and preliminary sampling. All cores from Holes 1002A through 1002E were processed through the MST track for measurements of magnetic susceptibility and GRAPE values, but cores from Holes 1002D and 1002E were packed and stored under refrigerated conditions without splitting them. All cores from Site 1002 were then shipped to the Gulf Coast Repository at Texas A&M University, where a special post-cruise sampling party later met from 28 May to 2 June 1996, to open, describe, and sample them. Though barrel sheets for cores from Holes 1002D and 1002E are included in this site chapter, the data and discussion presented here are based primarily upon shipboard observations and only the most general conclusions can be drawn.

SEISMIC STRATIGRAPHY

Site 1002 is located at 10°42.37′N, 65°10.18′W in the Cariaco Basin in a water depth of 893 m. Site 1002 was targeted to recover a high-deposition-rate, upper Quaternary sequence essentially duplicating that rotary cored at Site 147. Both sites are situated on the western edge of the central saddle that effectively divides the Cariaco Basin into two smaller sub-basins. Previous piston coring on numerous expeditions has shown that sedimentation on the saddle is largely continuous and undisturbed, whereas sedimentation on the deep sub-basin floors is dominated by turbidite deposition and slumping.

Site survey data used to target Site 1002 were collected on Leg 7 of the PLUME Expedition (*Thomas Washington*) in 1990. The complete trackline for the PLUME-7 survey is shown in Figure 3, whereas operational details can be found in the "Underway Geophysics and Pre-Site Surveys" section of the "Explanatory Notes" chapter (this volume). Site 1002 was drilled on an east-west single-channel seismic line between waypoints W-1 and X-1 (Fig. 4; see Fig. 3 for location). To ensure that Site 1002 was not placed too close to the western edge of the saddle, the site was approached along the corresponding PLUME-7 3.5-kHz line from the west, following the topography to the top of the slope using the 3.5-kHz system on board the *JOIDES Resolution.*

Site 1002 was cored with the APC to a maximum depth of 170.1 mbsf in Hole 1002C, terminating at a hard dolomite layer at that depth. It is likely that this and other semilithified dolomite layers (see "Lithostratigraphy" section, this chapter) are responsible for many of the prominent sub-bottom reflectors observed at this site. Once an integrated stratigraphy is completed for this site, based on isotope and biostratigraphic data, a more complete analysis of the seismic stratigraphic record at Site 1002 can, and will, be undertaken.

OPERATIONS

The 635-nmi transit from Site 1001 was made at an average speed of 10.5 kt. While on route to the site, two Venezuelan observers arrived by helicopter, and the Honduran observer and the JOIDES scientist departed. We conducted a short site survey with the 3.5-kHz echo sounder on approach to the site to verify that the site was properly located on the proposed local topographic high. Five holes were drilled (Table 1), with each hole being offset by about 15 m east of the previous hole.

Holes 1002A and 1002B

Hole 1002A was spudded with the APC system at 0.7 mbsf. The core liner was full (102.7% recovery), but did not contain a mudline, which necessitated spudding Hole 1002B. Hole 1002B recovered 6.2 m of sediment, including the mudline.

Hole 1002C

The APC system performed very well, with 109.1% average recovery for the hole. Cores 165-1002C-12H through 18H suffered from flow-in disturbance in the lower 2 to 3 m of each core. The liner for Core 165-1002C-18H was severely damaged, and the core had to be pumped out of the core barrel, though 9.92 m of sediment was still recovered. Core 165-1002C-19H also returned to the surface shattered, but this time only 0.15 m of sediment and hard dolomite was recovered.

Holes 1002D and 1002E

The APC/XCB coring systems were used for Holes 1002D and 1002E. Hole 1002D was spudded with the drill string 3 m higher than that used at Hole 1002C, and Hole 1002E was offset another 3 m, in order to offset core breaks. The XCB system was used after Cores 165-1002D-12H and 165-1002E-13H to avoid the flow-in problem and to penetrate the dolomite lenses more easily. Recovery was very good for both holes, averaging over 105% for the APC portions and over 70% for the XCB portions. Coring operations for both holes were halted just above the hard dolomite encountered in Core 165-1002C-19H to avoid penetrating any potentially dangerous gas pockets. There was concern that hydrocarbons and H_2S gas could be a problem at Site 1002; extra preparation and precautions were taken, though no significant problems were encountered during operations.

LITHOSTRATIGRAPHY

Site 1002 consists of a series of five holes drilled into the thick upper Quaternary sequence that sits atop the central saddle in the Cariaco Basin. Holes 1002A and 1002B were single mudline cores that were dedicated entirely to high-resolution interstitial water and geochemical sampling aboard ship. Cores from Hole 1002C, which terminated at a depth of 170.1 mbsf, were opened for preliminary shipboard description, whereas cores from Holes 1002D and 1002E were boxed as whole-round sections for transport back to the ODP Gulf Coast Repository. These latter cores were subsequently split and

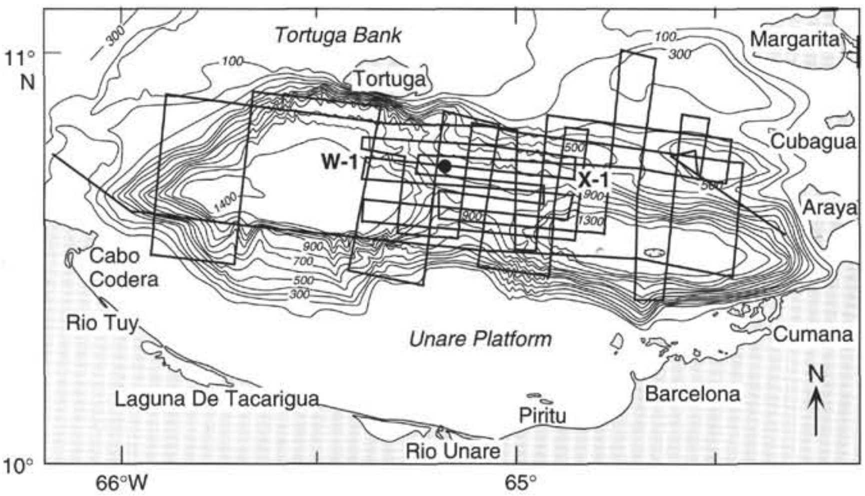

Figure 3. Location of Cariaco Basin Site 1002 in relation to tracklines from PLUME-7 pre-cruise site survey (*Thomas Washington*). Site 1002 is located on west-east trackline W-1/X-1 at the approximate position of DSDP Site 147.

described at a special post-cruise sampling party held in College Station from 28 May to 2 June 1996. Although VCDs for the cores from Holes 1002D and 1002E are presented in the "Cores" section, and the stratigraphic distribution of subunits in these holes is indicated in this section, sediment descriptions provided here are largely based on cores from Hole 1002C, and thus must be considered as preliminary.

The upper Quaternary sequence at Site 1002 is generally dominated by terrigenous sediment components with variable biogenic contributions of nannofossils, diatoms, and foraminifers. Much of the sediment is laminated, indicating deposition under largely anoxic conditions. Because no major changes in bulk sediment composition occur over the interval drilled, the sediments at Site 1002 are considered to form one formal lithologic unit. The sequence is divided into eight subunits based primarily on an apparent repetition of three major lithologies (Fig. 5). Subunits described here should be taken as a guide to average sediment composition with the realization that significant variability among sediment components can occur over scales of meters to millimeters.

As at other sites, measurements of digital color reflectance (see Appendix tables on CD-ROM in the back pocket of this volume for complete data set), magnetic susceptibility, and GRAPE values were taken, though here at Site 1002 at a higher resolution of 2-cm intervals. These data will be used for interhole correlations and for the post-cruise development of a composite depth section for the site. Magnetic susceptibility and reflectance data for the "green" (550 nm) wavelength from Hole 1002C are presented for general comparison with subunit lithologies in Figure 6, but time constraints and the current lack of stratigraphic information prevent a careful analysis of their significance.

Description of Lithologic Units

Unit I

Intervals: Cores 165-1002C-1H through 19H; Cores 165-1002D-1H through 18X; Cores 165-1002E-1H through 18X
Age: Holocene to late Pleistocene
Depth: 0.0–170.1 mbsf, Hole 1002C; 0.0–166.8 mbsf, Hole 1002D; 0.0–164.0 mbsf, Hole 1002E

The sediments at Site 1002 are primarily olive gray to greenish gray nannofossil silty clays, with minor but stratigraphically significant intervals rich in clays, diatoms, and foraminifers. Small, but persistent, contributions come from sponge spicules, quartz, mica, fish debris, ostracodes, molluscan debris, amorphous organic matter, and framboidal pyrite. Much of the sedimentary sequence is laminated, though laminae style appears to vary with depth and time. Eight subunits have been identified based on the alternation of a limited number of distinctive lithologies.

Subunit IA

Intervals: Sections 165-1002C-1H-1, 0 cm, through 1H-5, 43 cm; Sections 165-1002D-1H-1, 0 cm, through 2H-1, 80 cm; Sections 165-1002E-1H-1, 0 cm, through 2H-3, 101 cm
Age: Holocene to late Pleistocene
Depth: 0.0–6.43 mbsf, Hole 1002C; 0.0–5.50 mbsf, Hole 1002D; 0.0–5.81 mbsf, Hole 1002E

Subunit IA consists of silty clay with nannofossils and foraminifers that grade downward into diatom nannofossil clayey mixed sediment. The sediments are dark olive gray in color, undisturbed from bioturbation, and weakly to distinctly laminated throughout. Laminae are generally millimeter scale in thickness and are thicker and more easily visible where diatoms make up a significant component of the sediment (up to ~25%). Pteropods are very common on the split-core surface, both as fragments and as nearly whole individuals. Several thin (~1 cm), silty turbidites occur near the base of the subunit in each of the holes. The boundary between Subunits IA and IB marks the most recent onset of anoxic depositional conditions in the Cariaco Basin.

Subunit IB

Intervals: Sections 165-1002C-1H-5, 43 cm, through 2H-1, 11 cm; Sections 165-1002D-2H-1, 80 cm, through 2H-2, 120 cm; Sections 165-1002E-2H-3, 101 cm, through 2H-4, 127 cm
Age: late Pleistocene
Depth: 6.43–8.51 mbsf, Hole 1002C; 5.50–7.40 mbsf, Hole 1002D; 5.81–7.57 mbsf, Hole 1002E

Subunit IB consists of a thin, colorful mixture of fine-grained clay that underlies the laminated sediments of Subunit IA. The clay is mottled and shows evidence of bioturbation, indicating deposition under oxic conditions. Immediately beneath the base of Subunit IA, the clays are light gray to light greenish gray in color, blending below to yellowish brown and light reddish brown. Nannofossils and foraminifers are present, but in low apparent abundance relative to terrigenous components, whereas diatoms are absent. Pyrite is common in both framboidal and disseminated form.

Subunit IC

Intervals: Sections 165-1002C-2H-1, 11 cm, through 5H-6, 90 cm; Sections 165-1002D-2H-2, 120 cm, through 6H-1, 109 cm; Sections 165-1002E-2H-4, 127 cm, through 6H-3, 112 cm
Age: late Pleistocene
Depth: 8.51–45.30 mbsf, Hole 1002C; 7.40–43.79 mbsf, Hole 1002D; 7.57–43.92 mbsf, Hole 1002E

Subunit IC consists of just over 36 m of olive gray to light olive gray nannofossil silty clay. Much of the sequence is laminated (Fig.

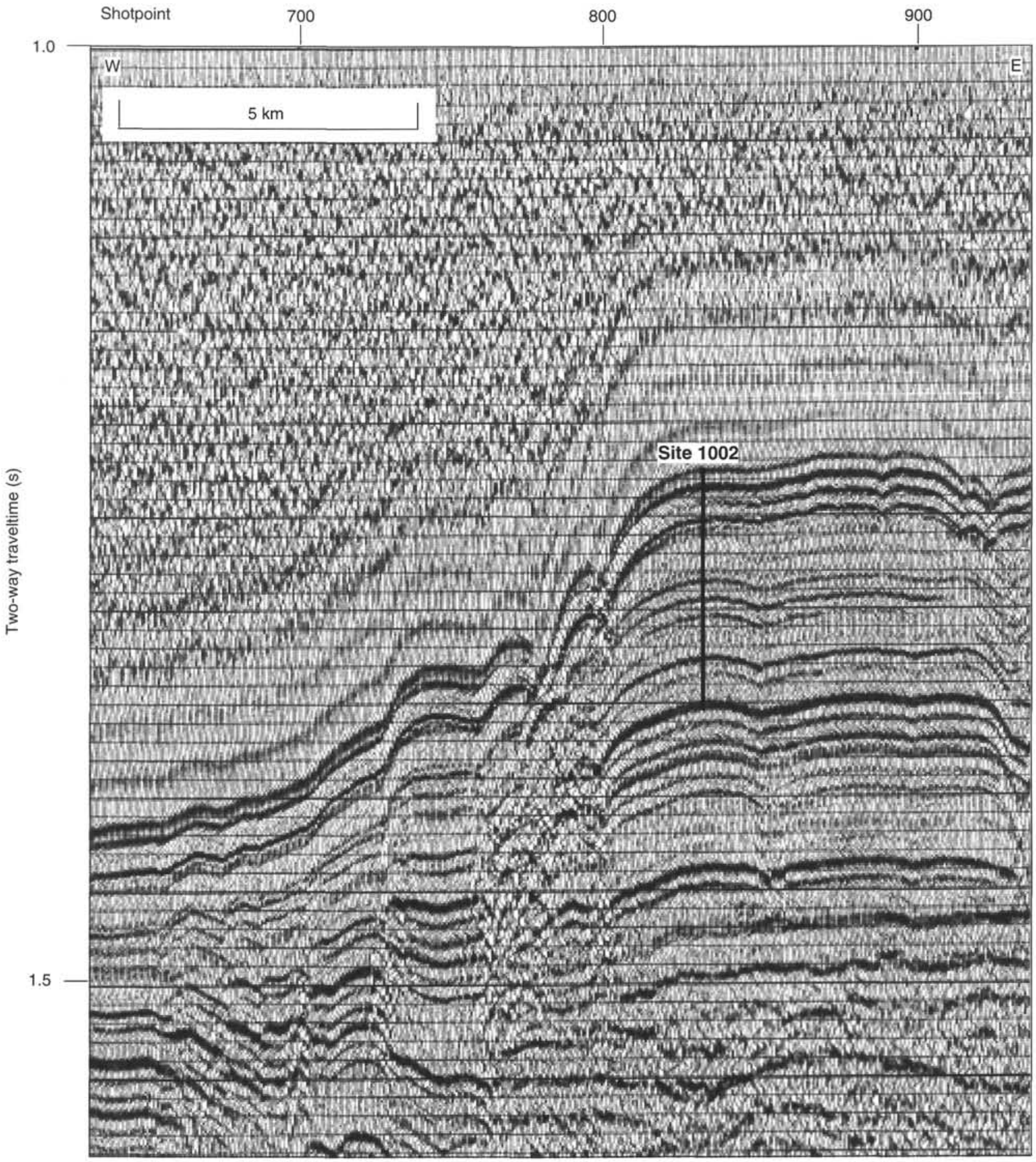

Figure 4. West-east single-channel seismic line from PLUME-7 site survey cruise showing location of Cariaco Basin Site 1002 at shotpoint 820. The location of this line is shown in Figure 3.

6; Table 2), with millimeter-scale laminations superimposed on faint color banding on the meter and submeter scale. Laminae vary from faint to well developed, alternating with massive, slightly bioturbated intervals. Laminae in Subunit IC differ in appearance from laminae of Subunit IA, with the presence of thin, gray silty layers lending to the contrast with the darker background sediment. Although a few of these silty layers clearly have turbidite origins, the majority show no evidence of redeposition and may instead reflect increased pulses of terrigenous input, presumably during the summer rainy season. The biogenic component of the laminae appears to be dominated by nannofossils, though foraminifers are generally more abundant near the base of the subunit and give the sediment a slightly coarser texture. The first downhole occurrence of dolomite at this site is observed in this subunit at a depth of 28.3 mbsf in Hole 1002C in the form of a well-indurated layer found at Section 165-1002C-4H-1, 86–92 cm. This layer appears to correlate with dolomite horizons observed in

Table 1. Coring summary, Site 1002.

Core no.	Date (Feb. 1996)	Time (UTC)	Depth (mbsf)	Cored (m)	Recovered (m)	Recovery (%)
165-1002A-						
1H	14	0100	0.0–9.5	9.5	9.77	103.0
Coring totals				9.5	9.77	103.0
165-1002B-						
1H	14	0130	0.0–6.2	6.2	6.24	100.0
Coring totals				6.2	6.24	100.0
165-1002C-						
1H	14	0220	0.0–8.4	8.4	8.37	99.6
2H	14	0300	8.4–17.9	9.5	9.73	102.0
3H	14	0320	17.9–27.4	9.5	9.89	104.0
4H	14	0340	27.4–36.9	9.5	9.76	103.0
5H	14	0400	36.9–46.4	9.5	10.12	106.5
6H	14	0440	46.4–55.9	9.5	10.21	107.5
7H	14	0510	55.9–65.4	9.5	11.15	117.3
8H	14	0540	65.4–74.9	9.5	10.91	114.8
9H	14	0745	74.9–84.4	9.5	9.83	103.0
10H	14	0825	84.4–93.9	9.5	10.91	114.8
11H	14	0845	93.9–103.4	9.5	10.11	106.4
12H	14	0930	103.4–112.9	9.5	11.15	117.3
13H	14	1000	112.9–122.4	9.5	10.87	114.4
14H	14	1030	122.4–131.9	9.5	10.75	113.1
15H	14	1100	131.9–141.4	9.5	10.93	115.0
16H	14	1130	141.4–150.9	9.5	10.83	114.0
17H	14	1200	150.9–160.4	9.5	9.82	103.0
18H	14	1220	160.4–169.9	9.5	9.92	104.0
19H	14	1245	169.9–170.1	0.2	0.15	75.0
Coring totals				170.1	185.71	109.2
165-1002D-						
1H	14	1530	0.0–4.7	4.7	4.70	100.0
2H	14	1600	4.7–14.2	9.5	9.46	99.6
3H	14	1620	14.2–23.7	9.5	9.98	105.0
4H	14	1650	23.7–33.2	9.5	9.94	104.0
5H	14	1725	33.2–42.7	9.5	10.03	105.6
6H	14	1750	42.7–52.2	9.5	10.23	107.7
7H	14	1815	52.2–61.7	9.5	11.11	116.9
8H	14	1845	61.7–71.2	9.5	11.05	116.3
9H	14	1915	71.2–80.7	9.5	11.32	119.1
10H	14	1945	80.7–90.2	9.5	10.65	112.1
11H	14	2015	90.2–99.7	9.5	10.66	112.2
12H	14	2100	99.7–109.2	9.5	11.24	118.3
13X	14	2220	109.2–118.6	9.4	0.00	0.0
14X	14	2310	118.6–128.2	9.6	8.26	86.0
15X	14	2345	128.2–137.8	9.6	9.65	100.0
16X	15	0020	137.8–147.4	9.6	8.06	83.9
17X	15	0055	147.4–157.1	9.7	9.05	93.3
18X	15	0130	157.1–166.8	9.7	6.80	70.1
Coring totals				166.8	162.19	97.2
165-1002E-						
1H	15	0330	0.0–1.8	1.8	1.81	100.0
2H	15	0350	1.8–11.3	9.5	10.02	105.5
3H	15	0410	11.3–20.8	9.5	9.58	101.0
4H	15	0445	20.8–30.3	9.5	8.97	94.4
5H	15	0520	30.3–39.8	9.5	9.87	104.0
6H	15	0550	39.8–49.3	9.5	10.32	108.6
7H	15	0615	49.3–58.8	9.5	10.44	109.9
8H	15	0645	58.8–68.3	9.5	10.61	111.7
9H	15	0715	68.3–77.8	9.5	10.07	106.0
10H	15	0745	77.8–87.3	9.5	8.73	91.9
11H	15	0815	87.3–96.8	9.5	10.92	114.9
12H	15	0845	96.8–106.3	9.5	10.38	109.2
13H	15	0915	106.3–115.8	9.5	10.65	112.1
14X	15	1000	115.8–125.4	9.6	6.25	65.1
15X	15	1040	125.4–135.0	9.6	9.72	101.0
16X	15	1115	135.0–144.6	9.6	8.89	92.6
17X	15	1200	144.6–154.3	9.7	8.81	90.8
18X	15	1230	154.3–164.0	9.7	8.84	91.1
Coring totals				164.0	164.88	100.5

Note: An expanded version of this coring summary table that includes lengths and depths of sections, location of whole-round samples, and comments on sampling disturbance is included on CD-ROM in the back pocket of this volume.

similar stratigraphic positions in Sections 165-1002D-4H-3, 57–60 and 77–82 cm, and 165-1002E-4H-5, 33–36 and 46–69 cm. Bivalve fragments, fish debris (bones and teeth), and pteropods can be observed on split-core surfaces throughout the subunit, whereas pyrite is present in both disseminated form and as well-preserved framboids.

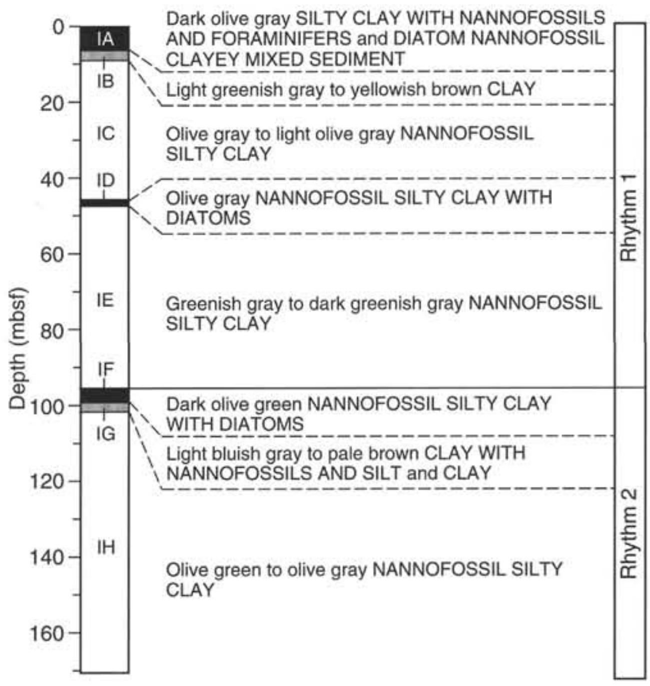

Figure 5. Generalized lithologic column showing subunits described from Hole 1002C, Cariaco Basin. The sequence of lithologies alternates in a way that suggests sedimentary "rhythms," probably reflecting the influences of climate and sea level on sedimentation and oxygenation state in the basin.

Subunit ID

Intervals: Sections 165-1002C-5H-6, 90 cm, through 5H-7, 88 cm; Sections 165-1002D-6H-1, 109 cm, through 6H-2, 100 cm; Sections 165-1002E-6H-3, 112 cm, through 6H-4, 141 cm
Age: late Pleistocene
Depth: 45.30–46.78 mbsf, Hole 1002C; 43.79–45.20 mbsf, Hole 1002D; 43.92–45.71 mbsf, Hole 1002E

Subunit ID is a relatively thin (~1.5 m) and well-laminated unit that differs from laminated intervals in Subunits IC and IE above and below in that the laminae again contain a significant diatom component. The nannofossil silty clays with diatoms found here are olive gray in color and show no evidence of bioturbation. Laminae are millimeter scale and resemble in appearance those observed in the lower half of Subunit IA. Preliminary analysis of the diatom flora indicates that it consists of a mixture of taxa dominated by *Thalassionema* spp., a common oceanic upwelling form, and *Coscinodiscus.*

Subunit IE

Intervals: Sections 165-1002C-5H-7, 88 cm, through 11H-3, 0 cm; Sections 165-1002D-6H-2, 100 cm, through 11H-5, 0 cm; Sections 165-1002E-6H-4, 141 cm, through 12H-2, 0 cm
Age: late Pleistocene
Depth: 46.78–95.63 mbsf, Hole 1002C; 45.20–95.33 mbsf, Hole 1002D; 45.71–96.99 mbsf, Hole 1002E

Subunit IE consists of greenish gray to dark greenish gray nannofossil silty clay. Although this subunit is compositionally similar to Subunit IC, it is generally more massive with indications of slight bioturbation. Scattered shell material is observed on the split-core surface at various levels. Semilithified layers and nodules of dolomite are found in greater numbers in this subunit (Fig. 6). To a first approximation, these appear to occur in association with an interval of interbedded laminated and massive sediments centered on about 60 mbsf, perhaps suggesting that such youthful dolomite formation is

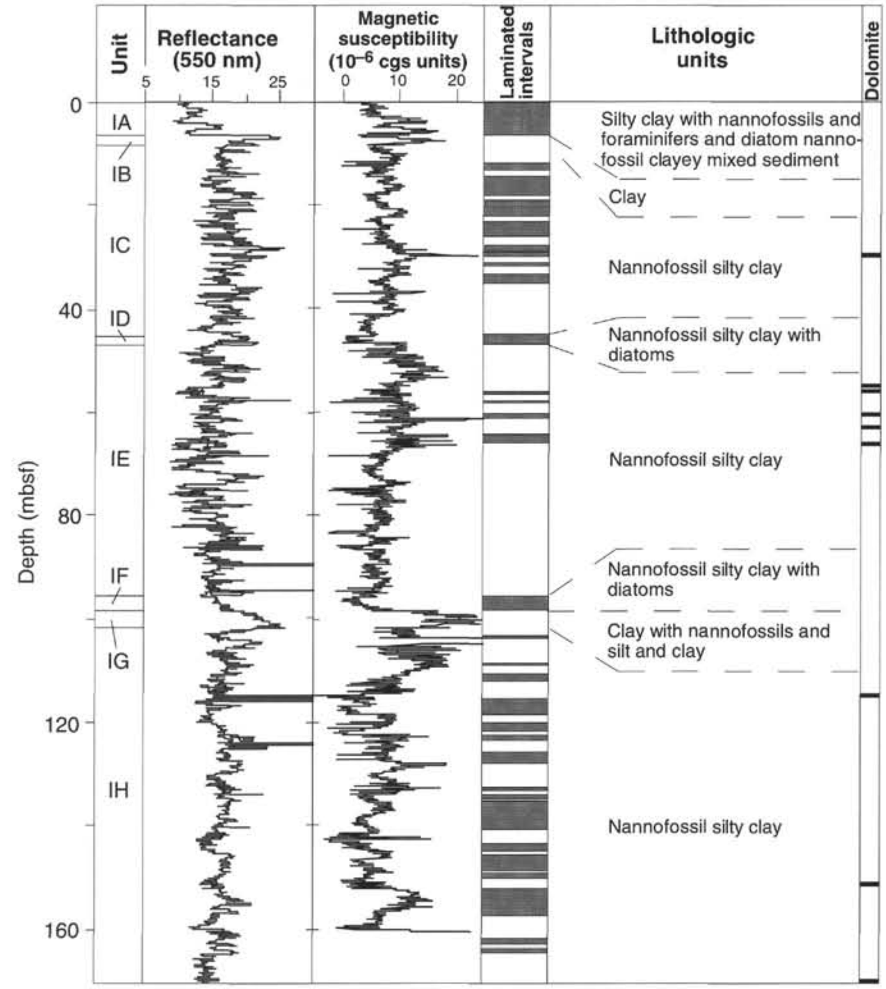

Figure 6. Comparison of Hole 1002C lithologic subunits with shipboard measurements of percent color reflectance in the 550-nm wave band ("green") and magnetic susceptibility. Also shown are a preliminary compilation of laminae distribution trends from visual shipboard observations (see Table 2), and the downhole distribution of semilithified to lithified dolomite layers. Laminae distribution patterns should be taken as preliminary as time constraints at sea precluded careful cleaning of the core surface before being described.

related to chemical changes that accompany transitions from oxic to anoxic conditions, or vice versa. Foraminifers are generally more abundant near the base of the subunit and give the sediment a slightly coarser texture.

Subunit IF

Intervals: Sections 165-1002C-11H-3, 0 cm, through 11H-5, 0 cm; Sections 165-1002D-11H-5, 0 cm, through 11H-6, 122 cm
Age: late Pleistocene
Depth: 95.63–98.63 mbsf, Hole 1002C; 95.33–98.05 mbsf, Hole 1002D

Subunit IF is a thin body of well-laminated (millimeter scale) sediments made up of nannofossil silty clay with diatoms. Compositionally, the sediments resemble those found in Subunits IA and ID, with diatoms primarily found within the lighter laminae. Sediments of Subunit IF are dark olive green in color and undisturbed by bioturbation. This subunit was not recognized in Hole 1002E, probably the result of a coring gap inferred near the top of Core 165-1002E-12H.

Subunit IG

Intervals: Sections 165-1002C-11H-5, 0 cm, through 11H-7, 15 cm; Sections 165-1002D-11H-6, 122 cm, through 11H-CC, 34 cm; Sections 165-1002E-12H-2, 0 cm, through 12H-4, 75 cm
Age: late Pleistocene
Depth: 98.63–101.78 mbsf, Hole 1002C; 98.05–99.70 mbsf, Hole 1002D; 96.99–100.74 mbsf, Hole 1002E

Subunit IG consists of approximately 3 m of fine-grained clay and clay with nannofossils and silt. The clays of this subunit form a colorful sequence of interbedded light bluish gray and pale brown layers that stand in stark contrast to the dark olive green sediments above and below. The sediments are generally massive with slight to moderate bioturbation. This subunit appears to be nearly identical in character and composition to Subunit IB, near the top of the Hole 1002C sequence.

Subunit IH

Intervals: Sections 165-1002C-11H-7, 15 cm, through 19H-CC, 15 cm; Sections 165-1002D-12H-1, 0 cm, through 18X-CC, 34 cm; Sections 165-1002E-12H-4, 75 cm, through 18X-CC, 36 cm
Age: late Pleistocene
Depth: 101.78–170.1 mbsf, Hole 1002C; 99.70–163.90 mbsf, Hole 1002D; 100.74–163.14 mbsf, Hole 1002E

The final subunit recognized in Hole 1002C is again a sequence of nannofossil silty clay, olive green to olive gray in color and commonly laminated. Laminations, where present, are generally thin and faintly visible. Their distribution alternates with more massive intervals that show evidence of slight bioturbation. Scattered shell material commonly occurs on split-core surfaces. During the coring operation in Hole 1002C, a hard, semilithified dolomite layer was recovered in Section 165-1002C-13H-7 at 130 cm. Incomplete stroke of the APC was experienced on each of Cores 165-1002C-12H through 18H in this hole, with flow-in generally affecting the bottom 1–3 m

Table 2. Preliminary compilation of laminae distribution at Site 1002, based on shipboard observations from Hole 1002C sediments.

Core, section, interval (cm)	Depth (mbsf)	Thickness (m)	Comments
1002C-1H-1, 0 to 1H-3, 128	0.00–4.28	4.28	Faint, millimeter scale in Section 3
1002C-1H-3, 128 to 1H-4, 100	4.28–5.50	1.22	Well developed, millimeter scale
1002C-1H-4, 100 to 1H-5, 43	5.50–6.43	0.93	Well developed, millimeter scale
1002C-2H-2, 16–22	10.06–10.12	0.06	Faint
1002C-2H-2, 104–108	10.94–10.98	0.04	Well developed
1002C-2H-3, 40 to 2H-4, 38	11.80–13.28	1.48	Faint, well developed between 30 and 38 cm in Section 165-1002C-2H-4; laminae slightly bioturbated
1002C-2H-3, 67–87	13.59–13.79	0.20	Faint
1002C-2H-3, 87–111	13.79–14.07	0.28	Laminated?
1002C-2H-5, 0 to 3H-1, 22	14.40–18.12	3.72	Decimeter-scale packets of faint and well-developed laminations
1002C-3H-1, 115 to 3H-2, 32	19.05–19.72	0.67	Well developed
1002C-3H-2, 32–82	19.72–20.22	0.50	Laminated?
1002C-3H-2, 82–131	20.22–20.71	0.49	Well developed
1002C-3H-3, 26–116	21.16–22.06	0.90	Well developed
1002C-3H-3, 116–131	22.06–22.21	0.15	Faint
1002C-3H-3, 131–145	22.21–22.35	0.14	Well developed; IW sample at 165-1002C-3H-3, 145–150 cm
1002C-3H-4, 75 to 3H-5, 130	23.15–25.20	2.05	Well developed. Silty-clay laminae commonest between 78 and 112 cm
1002C-3H-6, 0–79	25.40–26.19	0.79	Faint
1002C-3H-6, 79–146	26.19–26.86	0.67	Well developed
1002C-3H-7, 0–8	26.90–26.98	0.08	Faint
1002C-3H-7, 20–57	27.10–27.47	0.37	Well developed; between 1 and 4 mm thick
1002C-4H-1, 38–65	27.78–28.05	0.27	Well developed to faint
1002C-4H-1, 96–103	28.36–28.43	0.07	Faint
1002C-4H-1, 128–134	28.68–28.74	0.06	Faint
1002C-4H-2, 22–75	29.12–29.65	0.53	Faint
1002C-4H-3, 70–120	31.10–31.60	0.50	Faint
1002C-4H-5, 0–150	33.40–34.90	1.50	Faint
1002C-4H-6, 60–63	35.50–35.53	0.03	Faint
1002C-5H-2, 65–79	39.05–39.19	0.14	Faint
1002C-5H-6, 47–90	44.87–45.30	1.91	Faint
1002C-5H-6, 90 to 5H-7, 88	45.30–46.78	1.48	Well developed
1002C-6H-2, 36–40	47.03–47.07	0.04	Faint
1002C-6H-4, 34–41	50.01–50.08	0.07	Faint, millimeter scale
1002C-6H-4, 83–90	50.50–50.57	0.07	Well developed, millimeter scale
1002C-6H-4, 126–129	50.93–50.96	0.03	Faint, millimeter scale
1002C-7H-1, 37–77	56.27–56.67	0.40	Faint
1002C-7H-2, 105–128	57.83–58.06	0.23	Faint
1002C-7H-3, 78–109	59.06–59.37	0.31	Faint; upper 18 cm intermittently laminated
1002C-7H-4, 33–117	60.11–60.95	0.84	Faint; intermittent laminations
1002C-7H-5, 129–134	62.57–62.62	0.05	Faint
1002C-7H-7, 0 to 7H-8, 5	64.28–65.83	1.55	Faint
1002C-8H-4, 0–1	68.95–68.96	0.01	Faint
1002C-11H-3, 0 to 11H-4, 107	95.63–96.62	0.99	Faint
1002C-11H-3, 99 to 11H-4, 107	96.62–98.20	1.58	Well developed
1002C-11H-5, 105–110	99.68–99.73	0.05	Well developed
1002C-12H-1, 0–32	103.40–103.72	0.32	Faint
1002C-12H-4, 95–127	108.62–108.94	0.32	Faint
1002C-12H-6, 0–150	110.67–112.17	1.50	Faint
1002C-13H-3, 0 to 13H-4, 150	115.51–118.51	3.00	Faint
1002C-13H-6, 0 to 13H-7, 14	120.01–121.65	1.64	Faint to well developed; thickness range from 1 to 5 mm
1002C-13H-7, 100–130	122.51–122.81	0.30	Faint to well developed
1002C-14H-1, 21–59	122.61–123.01	0.40	Well developed
1002C-14H-2, 0–66	123.01–123.67	0.66	Well developed
1002C-14H-2, 120 to 14H-4, 150	125.70–128.00	2.30	Well developed (Section 2) to faint (Sections 3 and 4)
1002C-14H-5, 90–96	128.40–128.46	0.06	Faint
1002C-14H-5, 116–132	128.66–128.82	0.16	Faint
1002C-14H-6, 45–62	129.45–129.62	0.17	Faint
1002C-14H-6, 78–96	129.78–129.96	0.18	Faint
1002C-15H-2, 0–60	132.57–133.17	0.60	Faint
1002C-15H-3, 0–80	134.07–134.87	0.80	Faint
1002C-15H-3, 115 to 15H-7, 85	135.22–140.77	5.55	Faint (well developed in Section 6)
1002C-15H-8, 11–21	141.53–141.63	0.10	Faint
1002C-15H-8, 37–44	141.79–141.86	0.07	Faint
1002C-15H-8, 50–74	141.92–141.66	0.24	Faint
1002C-16H-2, 0–13	141.97–142.10	0.13	Faint to well developed
1002C-16H-2, 39–63	142.36–142.60	0.24	Faint
1002C-16H-3, 0–150	143.47–144.97	1.50	Faint
1002C-16H-4, 58 to 16H-6, 75	145.55–148.72	3.17	Well developed (Section 4); faint, thickness from 1 to 3 mm; slightly bioturbated
1002C-16H-6, 105 to 16H-7, 58	149.02–150.05	1.03	Faint
1002C-17H-1, 0–120	150.90–152.10	1.20	Faint
1002C-17H-2, 25–108	152.65–153.48	0.83	Faint
1002C-17H-3, 0–100	153.90–154.90	1.00	Faint
1002C-17H-4, 0–53	155.40–155.93	0.53	Faint
1002C-17H-5, 0–65	156.90–157.55	0.65	Faint
1002C-18H-2, 0–110	161.90–163.00	1.10	Faint
1002C-18H-2, 141–150	163.31–163.40	0.09	Well developed
1002C-18H-3, 0–50	163.40–163.90	0.50	Faint
1002C-18H-3, 122–150	164.62–164.90	0.28	Faint; intermittent lamination
1002C-18H-6, 24–38	167.12–167.26	0.14	Faint

of sediment. It was the driller's consensus that the coring was being impeded by additional hard, subsurface layers, presumably more layers of dolomite. Holes 1002D and 1002E were drilled therefore with the XCB below about 120 mbsf in order to recover more continuous and undisturbed sediment sequences. Subunit IG (and Hole 1002C) ends at 170.1 mbsf, the depth at which the APC was unable to penetrate an extremely hard dolomite layer, pieces of which were recovered in the core catcher of Core 165-1002C-19H. Holes 1002D and 1002E were offset successively shallower to offset core breaks and did not reach the dolomite layer that marks the base of this site.

Discussion

The sedimentary sequence at Site 1002 essentially duplicates the upper Quaternary section recovered at Site 147 at virtually the same location. However, in terms of recovery and core quality, there is almost no comparison between the two drilling efforts. Perhaps the best indication of the difference in quality is the fact that APC coring on Leg 165 has recovered a sequence that is laminated over much of its length, whereas Site 147 cores were so badly disturbed that laminae were only rarely found preserved.

Overall, the lithologic records at the two sites are very similar, as would be expected given their close proximity. Although cores from Site 147 were disturbed, thin layers of brown and gray clay similar to what were found near the surface were also identified at several deeper levels in the section. The DSDP Leg 15 scientists (Edgar, Saunders, et al., 1973) postulated that these deeper clays represented earlier periods of oxic conditions comparable with those observed during the last glacial maximum. They further suggested that sedimentation patterns in the Cariaco Basin followed a "rhythmic" alternation between periods of oxia and anoxia that were related to the glacial-interglacial cycles of the late Quaternary. The lack of good biostratigraphic datums over the interval of time represented by the sediments, however, prevented their association of these "rhythms" with specific climatic events.

At this early analytic stage of Leg 165, we can only say that Site 1002 sediments show similar evidence of large-scale sedimentary rhythms or cycles (Fig. 5). The larger "rhythms" seem to consist of a distinctive sequence of units, starting with deposition of nannofossil silty clays under mostly anoxic or near-anoxic conditions, followed by deposition of colorful, fine-grained, bluish gray and yellowish brown clays (e.g., Subunits IB and IG) under oxic bottom conditions. Culminating the sequence would be the deposition of a diatom-rich, distinctly laminated facies suggestive of strong upwelling conditions. Given this scenario, we are tempted to speculate, as the Leg 15 scientists did, that the transitions from earlier intervals of oxia to intervals of anoxia and high productivity represent periods of rapid deglaciation and sea-level rise, such as has been shown for the most recent deglaciation (Peterson et al., 1991). Under such circumstances, the abrupt transition between Subunits IG and IF at approximately 98 mbsf in Site 1002 might be assumed to reflect the rapid deglaciation at ~128 ka associated with the change from oxygen isotope Stages 6 to 5. Under periods of climate warming that are less extreme, an incomplete "rhythm" might develop, such as the interval represented by deposition of the diatom-rich Subunit ID, which lacks an underlying clay sequence. Again, it is possible to speculate that this interval might reflect the more subtle climate changes expected with the transition from oxygen isotope Stages 4 to 3. Further efforts to refine the stratigraphy of this site, particularly through the use of oxygen isotope stratigraphy, will allow testing of this and many other hypotheses in the months and years ahead.

BIOSTRATIGRAPHY

Calcareous Nannofossils

Standard smear slides were prepared from core catchers recovered in Hole 1002C. Nannofossils are abundant and mostly well preserved. Diversity tends to be low throughout the section, with species of *Gephyrocapsa* (largely *G. oceanica*) and *Emiliania huxleyi* dominating the assemblages. Relative abundance fluctuations of these species and of *Florisphaera profunda* were noted. The entire stratigraphic section at Site 1002 lies in the Quaternary calcareous nannofossil Zone CN15 of Okada and Bukry (1980), based on the occurrence of *E. huxleyi* in all samples. The age of the base of this zone is less than 0.248 Ma. Another potential marker, *Helicosphaera inversa,* the LO of which lies at 0.155 Ma (Sato et al., 1991), was observed in Sections 165-1002C-9H-CC, 11H-CC, and 13H-CC. The biostratigraphic potential of this species will be investigated in shore-based research.

Planktonic Foraminifers

Samples 165-1002C-1H-CC through 17H-CC were washed and examined. Planktonic foraminifer assemblages at Site 1002 include most species normally found in tropical oceans, except *Sphaeroidinella dehiscens.* However, temperate elements such as occasionally common *Globigerina bulloides, Globoconella inflata,* and *Neogloboquadrina pachyderma* (dextrally coiling) are also present. *Globigerina bulloides* was one of the most abundant species in some assemblages. The abundance of this species appears to vary inversely with respect to the abundance of *Globigerinoides ruber.* The morphologies of both species are unusually variable at Site 1002. The many forms of *G. bulloides* described and illustrated by Bolli and Premoli Silva (1973) are readily observed. Similarly, several specimens of *Globigerinoides ruber* were observed with two ultimate chambers or with the ultimate chamber centered over an earlier chamber (as in *Globigerinoides obliquus*) rather than over a suture.

Some species had discontinuous stratigraphic ranges. *Menardella menardii* is not present below Sample 165-1002C-12H-CC. *Neogloboquadrina pachyderma* is recorded only in Samples 165-1002B-1H-CC and 165-1002C-6H-CC, and is not observed below that level. *Pulleniatina obliquiloculata* is present in low numbers and in scattered samples. *Globorotalia tumida* is found in only three samples (165-1002C-1H-CC, 8H-CC, and 11H-CC), but the *flexuosa* form is not found above Sample 165-1002C-8H-CC. Therefore, a datum, the LO of *Globorotalia tumida flexuosa* at 0.08 Ma, can tentatively be placed in Core 165-1002C-8H. *Truncorotalia truncatulinoides* is present in most samples and is always dextrally coiled, except in Sample 165-1002C-17H-CC, where sinistrally coiled specimens are also found.

Foraminifer preservation is very good to good in all samples. Spines are rarely preserved on specimens, but tests are otherwise in good condition. Samples also include widely varying amounts and varieties of pteropods, pelecypods, ostracodes, benthic foraminifers, and fish teeth and vertebrae. Pyrite is frequently observed coating objects and filling voids.

PALEOMAGNETISM

The remanent magnetization of the archive-half sections of APC cores from Hole 1002C was measured using the pass-through cryogenic magnetometer at either a 5- or 10-cm interval. After measuring the natural remanent magnetization (NRM), the sections were partially demagnetized in a peak alternating field (AF) of 15 mT.

The NRM inclinations are generally strongly biased toward high positive inclinations (40°–80°) and are inconsistent with both the present-day geomagnetic field inclination (37°) and the expected axial dipole inclination (21°) for the latitude of the site (Fig. 7A). AF demagnetization generally reduces the inclinations to axial dipole for the upper 15 m of sediment, whereas below 15 m there are alternating intervals of higher than expected inclinations and intervals with values similar to those expected for an axial dipole (Fig. 7B). The observed directional results indicate that the drilling overprint observed at all previous sites is again present at Site 1002. AF demagnetization

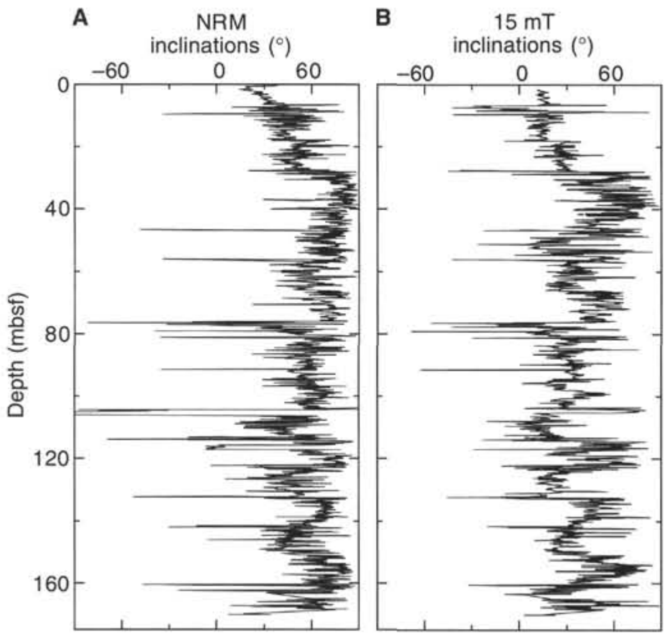

Figure 7. NRM inclinations and inclinations after 15-mT AF demagnetization of the archive-half sections of Hole 1002C.

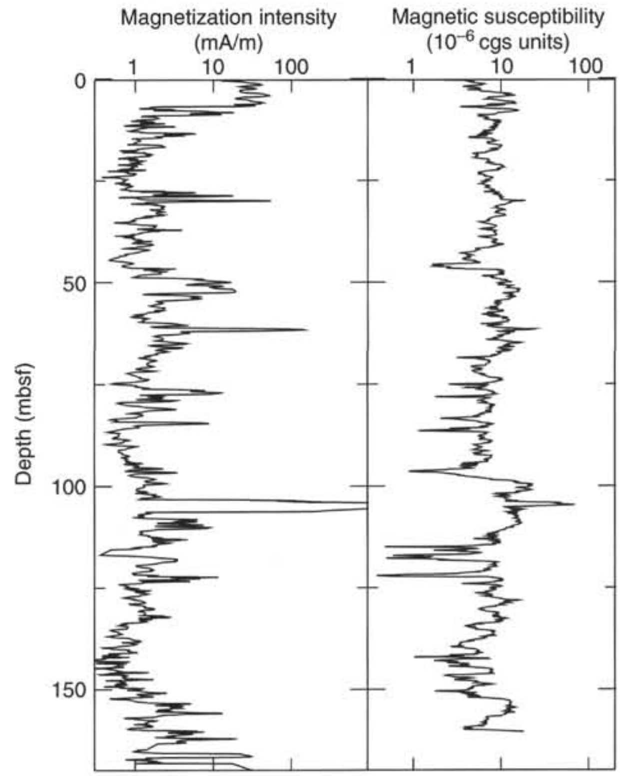

Figure 8. NRM intensity and magnetic susceptibility for Hole 1002C ($\log_{10}$ scale).

removes a significant portion of the secondary overprint, but the overprint is only removed completely in intervals that we speculate contain fine-grained magnetic material. We have planned post-cruise studies of subsamples to further assess demagnetization strategies for these sediments.

The NRM intensities after AF demagnetization at 15 mT range from 2 to 100 mA/m. Intervals of higher intensity are observed at depths of 0–7 (Holocene), 48–54, 98–123, and 150–170 mbsf (Fig. 8). In addition, higher susceptibility values are generally observed in the same intervals, and there is a general correspondence between the intensity and the susceptibility records (Fig 8). We speculate that the variations in intensity and susceptibility are related to glacial-interglacial cycles and that several cycles have been identified in Hole 1002C. We estimate that the bottom of Hole 1002C is within oxygen isotope Stage 7 and is estimated to be ~200 k.y., which gives an average sedimentation rate of ~850 m/m.y. for Hole 1002C.

ORGANIC GEOCHEMISTRY

Introduction

The tight time constraints at Site 1002 precluded detailed shipboard organic geochemistry. Shore-based studies are planned that address the character and temporal variability of the organic reservoir, as well as accumulation rates on a variety of time scales. Additional integrated studies will focus on the coupled organic-inorganic geochemical systems as they relate to pathways of organic remineralization and early diagenetic authigenesis under conditions of fluctuating depositional redox. In compliance with drilling safety requirements, headspace gases were analyzed routinely at a frequency of one per core for Hole 1002C, and one per section in Hole 1002B, a dedicated mudline core of ~6-m total length. Analytical details are discussed in the "Organic Geochemistry" section of the "Explanatory Notes" chapter (this volume).

Volatile Hydrocarbons

A comprehensive set of organic geochemical data for the Cariaco Basin is available for Site 147 of DSDP Leg 15. Total organic carbon (TOC) concentrations of up to 4 wt% were reported in this early study (Edgar, Saunders, et al., 1973). Subsequent work has revealed TOC levels in excess of these initial values (L. Peterson, pers. comm., 1996). Given the potential for organic enrichments, it is not surprising that gas-rich cores dominated the deep holes at Site 1002. The results for headspace volatile hydrocarbons are summarized in Table 3 and Figure 9. Methane dominated the headspace hydrocarbons in Hole 1002C, suggesting that methanogenesis is a major pathway of bacterial degradation under strongly reducing conditions. Nevertheless, low levels of C_2 through C_5 hydrocarbons were found at depths as shallow as Core 165-1002C-2H (<20 mbsf) and increased in concentration downcore. Because of the presence of thermogenic gases, we determined that a well-indurated, dolomitic horizon encountered (but not penetrated) at the base of Hole 1002C would not be drilled in the subsequent holes. A specific concern was the potential for an accumulation of upwardly migrating thermogenic hydrocarbons beneath an impermeable cap.

INORGANIC GEOCHEMISTRY

Seven interstitial water samples were collected at Site 1002 at depths from 13 to 157 mbsf in Hole 1002C (Table 4), providing low-resolution coverage throughout the entire cored section. A high-resolution study of the interval from 0 to 6 mbsf was also performed (dedicated Hole 1002B); these data will be presented elsewhere. Because of severe time constraints at the end of Leg 165, we were unable to analyze for the trace metals that require use of the AA spectrometer. Nonetheless, samples were analyzed for pH, salinity, chlorinity, alkalinity, sulfate, phosphate, ammonium, silica, Na, Mg, Ca, and K. Analytical methods are detailed in the "Inorganic Geochemistry" section of the "Explanatory Notes" chapter (this volume).

Data for Hole 1002C are presented in Table 4 and Figures 10–14. Downhole trends agree well with those published from DSDP Leg 15

Table 3. Concentrations of the dominant headspace hydrocarbon gases in Hole 1002C.

Core, section, interval (cm)	C1 (ppm)	C2 (ppm)	C3 (ppm)	I-C4 (ppm)	N-C4 (ppm)	I-C5 (ppm)	N-C5 (ppm)
165-1002C-							
1H-4, 0–5	30						
2H-4, 0–5	33492		4			1	
3H-4, 0–5	39243		5			1	
4H-4, 0–5	42282		2				
5H-4, 0–5	27155		4			2	
6H-6, 0–5	7970						
7H-4, 0–5	13576					1	
8H-7, 0–5	18125					1	
9H-6, 0–5	4186					7	1
10H-4, 0–5	16662		3			5	
11H-3, 0–5	9510		3				8
12H-4, 0–5	14705						
13H-4, 0–5	16434		8	3	2	10	1
14H-8, 0–5	9558					3	
15H-4, 0–5	16277		5			6	1
16H-7, 0–5	16894	47	11	4	3	14	2
17H-2, 0–5	15471	14	7	3	2	15	3

Notes: Concentrations are reported in parts per million (ppm). Concentrations below the limit of detection have been left blank.

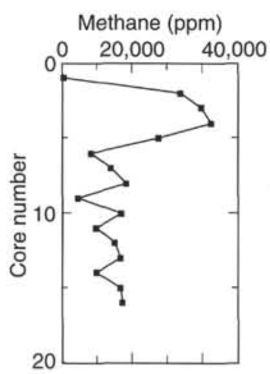

Figure 9. Methane concentrations in headspace gases from Hole 1002C.

(Gieskes, 1973) and are not discussed further at this point. There was no shipboard sediment chemistry program at Site 1002.

PHYSICAL PROPERTIES

The physical properties measurements at Site 1002 consisted only of scanning the cores with the multisensor track (MST). Magnetic susceptibility and GRAPE data were recorded at 2-cm intervals. Methods for these measurements are described in the "Physical Properties" section of the "Explanatory Notes" chapter (this volume). The magnetic susceptibility sample period was 5 s for Holes 1002A, 1002B, 1002C, and part of 1002D, but was reduced to 4 s for Sections 165-1002D-4H-2 to 165-1002E-18X-CC. The top and bottom 3 cm of each section were avoided for both the magnetic susceptibility and GRAPE measurements.

Because of time constraints, the magnetic susceptibility and GRAPE data have not been edited. Raw data from the MST measurements of Hole 1002C are presented in Figure 15, and all MST data are listed in Tables 5 and 6.

Preliminary examination of the first core from Holes 1002A, 1002B, and 1002C suggest that an excellent high-resolution correlation is possible between holes (Fig. 16). Discrepancies in the correlation may result from gas voids in the sections, which have very low magnetic susceptibilities and GRAPE densities, or a result of the 6-cm measurement gap that occurs between the tops and bottoms of adjacent sections.

SUMMARY AND CONCLUSIONS

Although understanding Caribbean ocean history was the common theme among the five sites drilled on Leg 165, Site 1002 differs significantly from other sites of this leg in the time scale of variability that its sediments record. In the Cariaco Basin, high sedimentation rates and a general absence of bioturbation have combined to produce a climatic and oceanographic record of nearly unparalleled resolution in the tropical ocean. Post-cruise studies of Site 1002 materials are expected to provide an important tropical counterpart to high-latitude ice cores for studies of large and abrupt climate changes in the latest Quaternary. Geochemical studies of this classic anoxic basin are also likely to yield important insights into the chemistry of anoxic systems and of the role of anoxia in the preservation and burial of organic carbon.

A total of five holes were drilled at Site 1002, two of which were mudline cores taken for geochemical studies, and three more taken for high-resolution paleoclimatic reconstructions. Only the cores from Hole 1002C were split onboard ship for preliminary descriptions and analysis. Time was short for inspection and discussion, and only the most preliminary observations can be made at this time.

Hole 1002C recovered a total of 170.1 m of mostly mixed hemipelagic sediments. The presence of *Emiliania huxleyi* at the base of the sequence suggests that all of the sediments fall within Zone CN15 or were deposited in the past 248,000 yr. This single biostratigraphic estimate is consistent with estimates based on extrapolating known sedimentation rates for the Holocene and the last glacial for the length of the drilled sequence.

Sediments in Hole 1002C are generally dominated by terrigenous components with variable biogenic contributions of nannofossils, diatoms, and foraminifers. Much of the sediment is laminated, indicating deposition under largely anoxic bioturbation-free conditions. Microbial methane is common, resulting in expanded sections and gas voids that developed in many of the cores upon retrieval. However, the quality and continuity of the cores appear to be very good to excellent as voids generally developed only along bedding surfaces.

The sedimentary sequence at Site 1002 was assigned to one formal lithostratigraphic unit and eight subunits. Despite this degree of subdivision, there appear to be only three major lithologies, which alternate in a semipredictable fashion. The bulk of the sequence consists of nannofossil silty clays, olive gray to greenish gray in color, which appear to have been deposited under both anoxic (laminated) and oxic (massive) conditions. These sediments are punctuated periodically by episodes of bluish gray and yellowish brown clay deposition, laid down under clearly oxic conditions. Generally following this, deposition of diatom-rich, distinctly laminated sediment indicates strong upwelling, such as was experienced during the early Holocene recorded by Subunit IB. Earlier periods of clay deposition, followed by the accumulation of diatom-rich sediments, may similarly signal earlier periods of deglaciation and sea level rise. Shore-based efforts to develop a stratigraphy for this site will allow testing of this hypothesis and will provide the basis for high- to ultra-high-resolution investigations of late Quaternary tropical paleoenvironments in the months and years ahead.

REFERENCES

Athearn, W.D., 1965. Sediment cores from the Cariaco Trench, Venezuela. *Tech. Rep.—Woods Hole Oceanogr. Inst.*, 65–37.

Bolli, H.M., and Premoli Silva, I., 1973. Oligocene to Recent planktonic foraminifera and stratigraphy of the Leg 15 sites in the Caribbean Sea. *In* Edgar, N.T., Saunders, J.B., et al., *Init. Repts. DSDP*, 15: Washington (U.S. Govt. Printing Office), 475–497.

Edgar, N.T., Saunders, J.B., et al., 1973. *Init. Repts. DSDP,* 15: Washington (U.S. Government Printing Office).

Ericson, D.B., and Wollin, G., 1968. Pleistocene climates and chronology in deep-sea sediments. *Science,* 162:1227–1234.

Gieskes, J.M., 1973. Interstitial water studies, Leg 15: alkalinity, pH, Mg, Ca, Si, PO_4, and NH_4. *In* Heezen, B.C., MacGregor, I.D., et al., *Init. Repts. DSDP,* 20: Washington (U.S. Govt. Printing Office), 813–829.

Hay, W.W., and Beaudry, F.M., 1973. Calcareous nannofossils–Leg 15, Deep Sea Drilling Project. *In* Edgar, N.T., Saunders, J.B., et al., *Init. Repts. DSDP,* 15: Washington (U.S. Govt. Printing Office), 625–683.

Heezen, B.C., Menzies, R.J., Broecker, W.S., and Ewing, M., 1958. Date of stagnation of the Cariaco Trench, southeast Caribbean. *Geol. Soc. Am. Bull.,* 69:1579. (Abstract)

Heezen, B.C., Menzies, R.J., Broecker, W.S., and Ewing, M., 1959. Stagnation of the Cariaco Trench. In *International Oceanographic Congress Preprints,* Sears, M. (Ed.): Washington (Amer. Assoc. Adv. Sci.), 99–102.

Hughen, K., Overpeck, J.T., Peterson, L.C., and Anderson, R.F., 1996. The nature of varved sedimentation in the Cariaco Basin, Venezuela, and its palaeoclimatic significance. *In* Kemp, A.E.S. (Ed.), *Palaeoclimatology and Palaeoceanography from Laminated Sediments,* Geol. Soc. Spec. Pub. London, 116:171–183.

Ladd, J.W., Holcombe, T.L., Westbrook, G.K., and Edgar, N.T., 1990. Caribbean marine geology: active margins of the plate boundary. *In* Dengo, G., and Case, J.E. (Eds.), *The Caribbean Region.* Geol. Soc. Am., Geol. of North Am. Ser., H:261–290.

Lidz, L., Charm, W.B., Ball, M.M., and Valdes, S., 1969. Marine basins off the coast of Venezuela. *Bull. Mar. Sci.,* 19:1–17.

Mann, P., Schubert, C., and Burke, K., 1990. Review of Caribbean neotectonics. *In* Dengo, G., and Case, J.E. (Eds.), *The Caribbean Region.* Geol. Soc. Am., Geol. of North Am. Ser., H:307–338.

Okada, H., and Bukry, D., 1980. Supplementary modification and introduction of code numbers to the low-latitude coccolith biostratigraphic zonation (Bukry, 1973; 1975). *Mar. Micropaleontol.,* 5:321–325.

Peterson, L.C., Overpeck, J.T., Kipp, N.G., and Imbrie, J., 1991. A high-resolution late Quaternary upwelling record from the anoxic Cariaco Basin, Venezuela. *Paleoceanography,* 6:99–119.

Richards, F.A., 1975. The Cariaco Basin (Trench). *Annu. Rev. Oceanogr. Mar. Biol.,* 13:11–67.

Rögl, F., and Bolli, H.M., 1973. Holocene to Pleistocene planktonic foraminifera of Leg 15, Site 147 (Cariaco Basin [Trench], Caribbean Sea) and their climatic interpretation. *In* Edgar, N.T., Saunders, J.B., et al., *Init. Repts. DSDP,* 15: Washington (U.S. Govt. Printing Office), 553–615.

Sato, T., Kameo, K., and Takayama, T., 1991. Coccolith biostratigraphy of the Arabian Sea. *In* Prell, W.L., Niitsuma, N., et al., *Proc. ODP, Sci. Results,* 117: College Station, TX (Ocean Drilling Program), 37–54.

Schubert, C., 1982. Origin of Cariaco Basin, southern Caribbean Sea. *Mar. Geol.,* 47:345–360.

Ms 165IR-107

NOTE: Core-description forms ("barrel sheets") and core photographs can be found in Section 4, beginning on page 403. Forms containing smear-slide data can be found in Section 5, beginning on page 821. Thin-section descriptions are given in Sections 6 and 7, beginning on page 851. See Table of Contents for material contained on CD-ROM.

Table 4. Interstitial water composition, Hole 1002C.

Core, section, interval (cm)	pH	Alkalinity (mM)	Salinity (g/kg)	Cl^- (mM)	Na^+ (mM)	Mg^{2+} (mM)	Ca^{2+} (mM)	SO_4^{2-} (mM)	NH_4^+ (μM)	PO_4^{3-} (μM)	$Si(OH)_4$ (μM)	K^+ (mM)
165-1002C-												
1H-3, 145–150	7.47	19.50	34	580	470	47.7	4.87	7.24	2135	66	1093	10.3
3H-3, 145–150	7.49	14.07	33	584	469	38.3	5.26	0.32	2871	12	795	9.6
6H-5, 150–155	7.84	11.38	32	574	476	28.1	4.06	BDL	4158	5	175	10.7
9H-5, 145–150	7.41	25.50	32	548	470	25.5	5.84	0.77	NA	7	313	11.7
12H-3, 145–150	7.83	29.40	31.5	534	458	24.6	4.06	0.57	7268	6	164	12.3
15H-6, 130–135	7.57	22.30	30	525	448	21.0	3.99	0.00	9894	13	543	10.7
17H-4, 150–156	7.92	17.41	30	522	446	19.0	2.79	0.18	7735	5	84	12.3

Notes: BDL = below detection limit, NA = not analyzed. This entire table also appears on CD-ROM (back pocket).

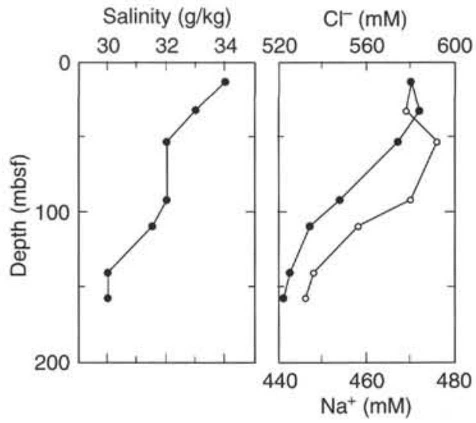

Figure 10. Depth profiles of salinity, Na^+ (open circles), and Cl^- (solid circles) in Site 1002 interstitial waters.

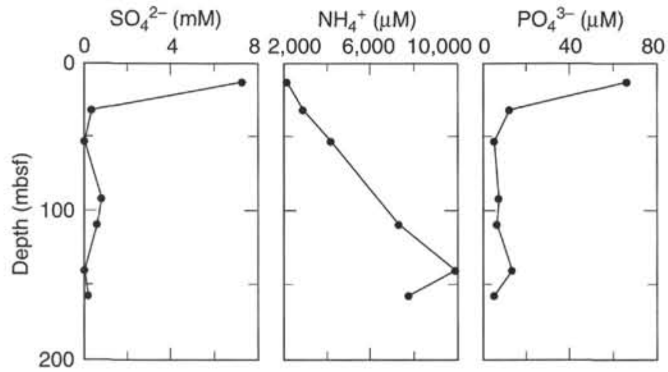

Figure 11. Depth profiles of SO_4^{2-}, NH_4^+, and PO_4^{3-} in Site 1002 interstitial waters.

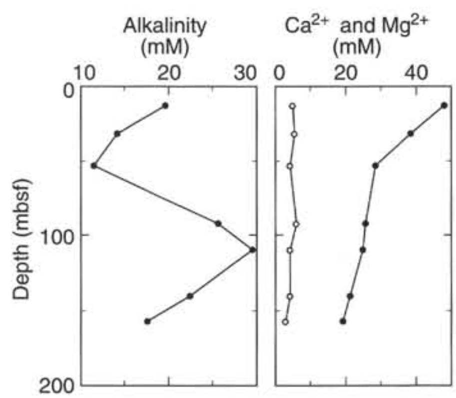

Figure 12. Depth profiles of alkalinity, Ca^{2+} (open circles), and Mg^{2+} (solid circles) in Site 1002 interstitial waters.

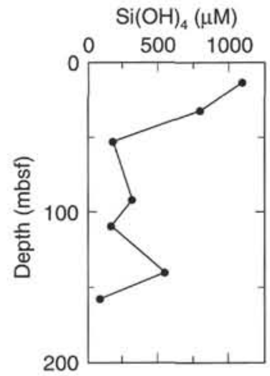

Figure 13. Depth profile of silica in Site 1002 interstitial waters.

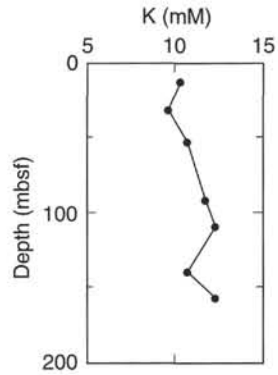

Figure 14. Depth profile of K in Site 1002 interstitial waters.

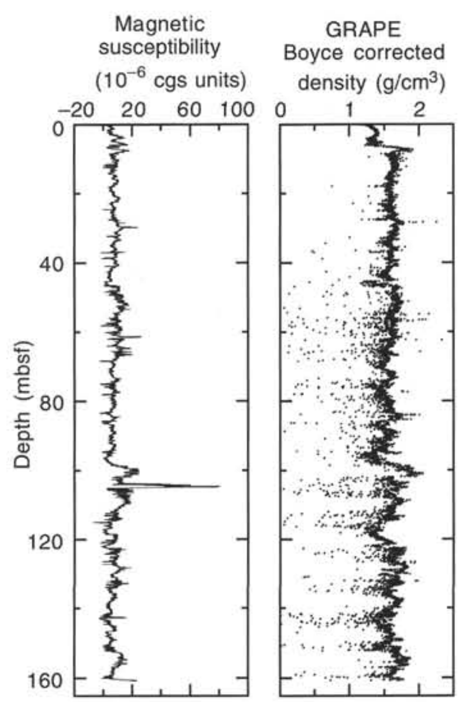

Figure 15. Multisensor track data showing magnetic susceptibility and GRAPE density for Hole 1002C.

Table 5. Gamma-ray attenuation porosity evaluator (GRAPE) data for Site 1002.

Core, section, interval (cm)	Depth (mbsf)	Raw counts	DAQ period (s)	Density (g/cm^3)	Boyce corr. density (g/cm^3)
165-1002A-					
1H-1, 3	0.03	25728	3	1.292	1.19244
1H-1, 5	0.05	24970	3	1.349	1.25343
1H-1, 7	0.07	25378	3	1.318	1.22026
1H-1, 9	0.09	24995	3	1.347	1.25129
1H-1, 11	0.11	24625	3	1.375	1.28125
1H-1, 13	0.13	24909	3	1.354	1.25878
1H-1, 15	0.15	24381	3	1.394	1.30158
1H-1, 17	0.17	24490	3	1.386	1.29302
1H-1, 19	0.19	24478	3	1.387	1.29409
1H-1, 21	0.21	24394	3	1.393	1.30051

Notes: DAQ = data acquisition. Density = bulk density. Corr. = correction. The data in this table differ from the raw data in that (1) all columns do not appear, (2) depths have been added, and (3) columns have been labeled.

Only part of this table is produced here. The entire table appears on CD-ROM (back pocket).

Table 6. Magnetic susceptibility data for Site 1002.

Core, section, interval (cm)	Depth (mbsf)	Raw mean susc. (10^{-6} cgs)	SD susc.	Drift corr.	DAQ period (s)	Bkgd. corr.
165-1002A-						
1H-1, 3	0.03	2.8	0.55472	0	5	–0.043
1H-1, 5	0.05	3.6	0.547848	–0.1	5	–0.069
1H-1, 7	0.07	3	0.79636	–0.1	5	–0.094
1H-1, 9	0.09	3.2	0.980361	–0.1	5	–0.119
1H-1, 11	0.11	4.2	0.32	–0.1	5	–0.144
1H-1, 13	0.13	5.2	0.872731	–0.2	5	–0.17
1H-1, 15	0.15	5.8	0.983819	–0.2	5	–0.195
1H-1, 17	0.17	4.2	0.817251	–0.2	5	–0.221
1H-1, 19	0.19	4.8	0.790591	–0.2	5	–0.246
1H-1, 21	0.21	4.2	1.1853	–0.3	5	–0.271

Notes: susc. = susceptibility, SD = standard deviation, corr. = correction, DAQ = data acquisition, and Bkgd. corr. = background correction. The data in this table differ from the raw data in that (1) all columns do not appear, (2) depths have been added, (3) columns have been labeled, and (4) magnetic susceptibility has been averaged.

Only part of this table is produced here. The entire table appears on CD-ROM (back pocket).

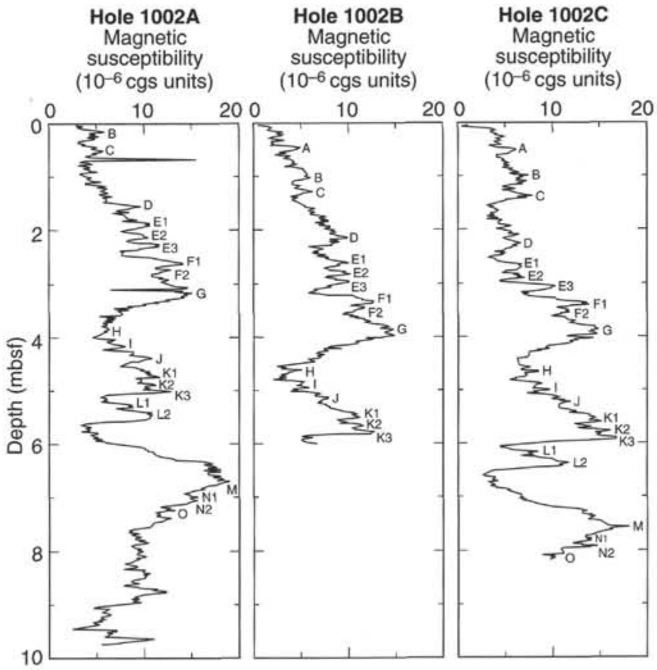

Figure 16. Magnetic susceptibility for the first cores of Holes 1002A, 1002B, and 1002C, and a preliminary correlation between the holes. The letters identifying various peaks are not meant to have any stratigraphic significance.